





[View Journal Online](#)  
[View Article Online](#)

# Overcoming multidrug-resistant bacteria and fungi by green synthesis of AgNPs using *Nepeta pogonosperma* extract, optimization, characterization and evaluation of antibacterial and antifungal effects

Mohammad Ali Ebrahimzadeh <sup>1</sup>, Amin Barani <sup>1</sup>, Amir Hossein Habibian <sup>2</sup>,  
 Hamid Reza Goli <sup>1</sup> and Seyedeh Roya Alizadeh <sup>1,\*</sup>

<sup>1</sup> Department of Medicinal Chemistry, School of Pharmacy and Pharmaceutical Sciences Research Center, Mazandaran University of Medical Sciences, Sari, 4847193698, Iran

<sup>2</sup> Pardis School of Pharmacy, Mazandaran University of Medical Sciences, Ramsar, 4691710001, Iran

\* Corresponding author at: Department of Medicinal Chemistry, School of Pharmacy and Pharmaceutical Sciences Research Center, Mazandaran University of Medical Sciences, Sari, 4847193698, Iran.

e-mail: [ro.alizadeh@mazums.ac.ir](mailto:ro.alizadeh@mazums.ac.ir) (S.R. Alizadeh).

## RESEARCH ARTICLE

## ABSTRACT



doi: 10.5155/eurjchem.14.2.254-263.2404

Received: 25 December 2022

Received in revised form: 07 February 2023

Accepted: 01 March 2023

Published online: 30 June 2023

Printed: 30 June 2023

## KEYWORDS

Green synthesis  
 Characterization  
 Antifungal activity  
 Silver nanoparticles  
 Antibacterial activity  
*Nepeta pogonosperma*

This study explained a green synthesis of silver nanoparticles (AgNPs) using *Nepeta pogonosperma* extract and evaluated their antibacterial activity. Optimization of the temperature, concentration, pH, and reaction time was established to produce silver nanoparticles. The best condition was 10 mM AgNO<sub>3</sub>, pH = 14, temperature 85 °C, and reaction time 24 hours. The formation of silver nanoparticles was confirmed by colour-changing, UV-vis, FE-SEM, EDX, XRD, FT-IR, and DLS analysis. The prepared AgNPs had a spherical shape with an average size of 51.21±0.02 nm. In addition, our biofabricated nanoparticles displayed potential antibacterial activity against the tested strains. The MIC value of 1.17 µg/mL was determined against strains of *Pseudomonas aeruginosa*, *Acinetobacter baumannii*, and *Escherichia coli* and 2.34 µg/mL against *Staphylococcus aureus*, *Klebsiella pneumoniae*, *Proteus mirabilis* and *Enterococcus faecalis*. Furthermore, AgNPs exhibited excellent antifungal effects against *Candida albicans* strains (0.073 µg/mL). In general, *N. pogonosperma* played an important role in reducing Ag(+1) to Ag(0) and the production of Ag(0) with suitable surface features in combination with efficient biological activities.

Cite this: *Eur. J. Chem.* 2023, 14(2), 254-263

Journal website: [www.eurjchem.com](http://www.eurjchem.com)

## 1. Introduction

In recent years, with the increase in population and the emergence of drug resistance in various fields, it has become an important and worrying issue. Globally, after cancer drug resistance, bacterial and infection drug resistance has the second rank [1-4]. Drug resistance is created due to the high, excessive, and arbitrary use of antibiotics and disinfectants and genetic changes in infectious agents. Pathogens and infectious agents that are exposed to anti-infective drugs can develop drug resistance and transfer it to new pathogen cells during cell division. In addition, resistance to an antibiotic may appear as resistance to other antibiotics with a similar structure, which causes multiple drug-resistant strains (MDR) [5]. It is predicted that by 2050, if no new drugs are synthesized, no effective antibiotics will be available to treat infections [6,7]. Alternative methods, including bacteriocins, essential oils (EOs), phage therapy, antibodies, quorum sensing inhibitors (QSI), and nanotherapy, have been studied and investigated in recent

years due to the enormous and high cost of discovering, developing, and producing new drugs [7,8].

Over time, nanotechnology and nanoscience have been used in different fields such as medicine, agriculture, biomedicine, pharmaceuticals, food technology, cosmetics, etc. [9,10]. Nanoparticles (NPs) can be manufactured using biological, physical, and chemical methods [4,11]. Chemical and physical methods have many disadvantages, such as high cost, low efficiency, the presence of toxic waste, and environmental pollution. In contrast, the biological method is cost-effective, environmentally friendly, fast, safe, and non-toxic [12-15]. Plants, bacteria, fungi, yeast, and algae can be used in biological methods for the synthesis of different NPs. Due to cross-contamination and significant problems in maintaining microorganisms to synthesize NPs, the best way to synthesize is the use of plants, which is called green synthesis [10]. Currently, various metal NPs, including CuO [16], TiO<sub>2</sub> [17], ZnO [17], MgO [18], Pt [19], Ag [20], Au [15] and Fe [14], have been synthesized using the green synthesis method. Among these

NPs, silver nanoparticles have received special attention from researchers because of their unique properties and applications. In this investigation, silver nanoparticles (AgNPs) were produced using the extract of the *Nepeta pogonosperma* plant (as a reducer, capping agent, and stabiliser) with the green synthesis method. *Nepeta L.* (from Lamiaceae) comprises approximately 300 species. Iran, with 75 species, is one of the sources of this genus. Extracts of many types of nepta are used in domestic medicine [21]. Several species are broadly employed in medications due to their expectorant, antiseptic, antitussive, antiasthmatic, and febrifuge properties. Furthermore, *N. meyeri* and *N. persica* have exhibited antimicrobial and anxiolytic properties [21]. In a study, the anti-inflammatory activity of essential oil, aerial parts, and hairy root extracts of *N. pogonosperma* was assessed on rat brain mixed cells; 0.5 µg/mL essential oil meaningfully reduced nitric oxide (NO) generation. By reviewing the research that has been carried out on the genus *Nepeta*, this genus contains more flavonoid compounds (the subgroup of flavones). Other compounds of this genus include iridoids, phenols, and diterpenes [22-24].

In this study, optimization and characterization of the prepared NPs using *N. pogonosperma* were performed. Several analytical techniques such as ultraviolet-visible (UV-vis) spectroscopy, scanning electron microscopy (SEM), energy-dispersive X-ray spectroscopy (EDX), X-ray diffraction analysis (XRD), dynamic light scattering (DLS), zeta potential, and Fourier transform infrared spectroscopy (FT-IR) proved the synthesized AgNPs. Due to the importance of multidrug resistance to chemical drugs, in order to solve this problem, many fungal and bacterial strains were used to investigate the antifungal and antibacterial effects of the nanoparticles synthesized through green synthesis. The choice of numerous bacteria and fungi is to investigate the inhibitory effects of nanoparticles more fully. Then, its antibacterial activity was studied against seven ATCC microorganisms and various multidrug-resistant bacteria isolated from a clinical specimen. In addition, our AgNPs were tested against several resistant fungi strains.

## 2. Experimental

### 2.1. Materials and characterization

The silver nitrate (AgNO<sub>3</sub>) and methanol solution were prepared by Sigma-Aldrich Company. The *N. pogonosperma* plant was collected from Alamut, Iran, and dried in the shade away from sunlight. The optimized green silver nanoparticles were analyzed using analytical methods, including UV/Vis spectrophotometer (T80 UV-Vis spectrophotometer, PGI, Beijing, China), FE-SEM and EDX (TESCAN BRNO-Mira3) and XRD (PANalytical X-PERT PRO diffractometer (2θ = 10 to 80°) with CuKα source (λ = 1.54 Å). FT-IR spectra were recorded by an ATR FT-IR spectrometer (Cary 630, Agilent, Santa Clara, CA, USA) from 4000 to 650 cm<sup>-1</sup>. We used DLS data obtained from Horiba-SZ-100-Z with a scattering angle of 90°, the holder temperature of 25.1 °C.

### 2.2. Preparation of *N. pogonosperma* extract

The plant was identified and collected from Alamut and then dried at room temperature. Then 100 g of crushed parts of the plant (whole plant) were extracted by the maceration method with methanol solvent for 24 hours at room temperature [14]. The extract solution was filtered with Whatman filter paper (Grade 41) with a pore size of 20 µm, and the extract obtained was dried at 60 °C by rotary (Hei zbad WB eoc, Germany) to obtain a solid extract. Finally, 10 g of dried solid extract was obtained to continue the steps.

### 2.3. Biosynthesis of silver nanoparticles (AgNPs)

In the typical synthesis of AgNPs, 12.5 mL of the extract solution with a concentration of 1 mg/mL (1 mg of methanolic extract dissolved in 1 mL of deionized water) was prepared at pH = 14 using NaOH 2 M (Solution I). A solution of AgNO<sub>3</sub> with a concentration of 10 mM was prepared at a temperature of 85 °C (Solution II). Then, while stirring, solution one was added drop by drop to solution two and stirred. The color change of the solution to dark brown due to the reduction of the Ag<sup>+</sup> ion to Ag<sup>0</sup> nanoparticles was observed and confirmed by a UV-vis spectrophotometer. The biosynthesized green nanoparticles were separated by centrifugation (3-30 k; SIGMA) at 14,000 rpm (20 min) and washed three times (with deionized water and methanol). The precipitate achieved was dried in an oven at 60 °C for 24 hours. Various experiments were performed to optimize and evaluate the effect of different parameters such as temperature, pH, silver nitrate concentration, and time on the production of silver nanoparticles in these experiments (Table 1). Optimized green AgNPs were analyzed using analytical methods and then used to evaluate biological tests.

### 2.4. Biological activities of the biosynthesized AgNPs

#### 2.4.1. Antibacterial activity

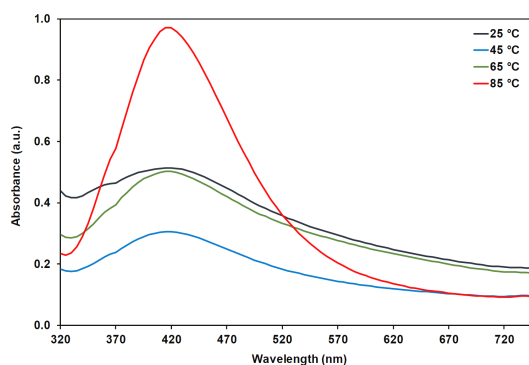
The Mueller Hinton broth (MHB) method was used to evaluate the antibacterial properties of AgNPs using the broth microdilution method [25]. Antibacterial evaluation was performed against seven ATCC strains and eight strains of clinically isolated bacteria resistant to the drug. Gram-negative and positive bacteria containing *Staphylococcus aureus* (*S. aureus*; ATCC 29213), *Acinetobacter baumannii* (*A. baumannii*; ATCC 19606), *Klebsiella pneumoniae* (*K. pneumoniae*, ATCC 700603), *Proteus mirabilis* (*P. mirabilis*; ATCC 25933), *Enterococcus faecalis* (*E. faecalis*; ATCC 29212), *Escherichia coli* (*E. coli*; ATCC 25922), and clinically isolates bacteria, including *S. aureus* (VRSA), *S. aureus* (MRSA), *E. faecalis*, *P. aeruginosa*, *A. baumannii*, *E. coli*, *K. pneumoniae* and *P. mirabilis* that supplied from The Microbiology Department of Mazandaran University of Medical Sciences (Iran). Ciprofloxacin was considered as a reference compound. In the process, 100 µL of MHB containing different concentrations of AgNPs was added to all wells. Then 100 µL of diluted bacterial suspension was entered into each well and the plates were incubated at 37 °C for 24 hours using natural convection incubators (BINDER Standard-Incubators, USA). Then, the minimum inhibitory concentration (MIC) value was determined for the prepared AgNPs. Subsequently, for the determination of the minimum bactericidal concentration (MBC), several MIC dilutions were cultured in Mueller Hinton agar culture medium for 24 h at 37 °C. After 24 hours, the lowest concentration that indicated that there was no visible growth in the plates was considered the MBC value [4,25].

#### 2.4.2. Antifungal activity

The antifungal activity of the synthesized green AgNPs was determined using the broth microdilution method. First, in a 96-well plate, 100 µL of synthesized Ag NP were loaded into well 1, then 100 µL of Roswell Park Memorial Institute (RPMI) was loaded into wells. Next, 100 µL of the contents of the first well were removed and added to the second well (this dilution of the concentration of synthesized nanoparticles serially continues). Then 100 µL of fungal suspension was added to the wells and incubated at 37 °C. Subsequently, the MIC values were evaluated for *Candida albicans* strains (IFRC1873 and IFRC1874), *Aspergillus fumigatus* (IFRC 1649), *Aspergillus fumigatus* (IFRC 1505), *Trichophyton mentagrophytes* (FR1 22130), *Trichophyton mentagrophytes* (FR5 22130), *Fusarium proliferatum* (IFRC 1871), *Fusarium equiseti* (IFRC 1872).

**Table 1.** Preparation conditions of samples.

Sample	Temperature (°C)	AgNO <sub>3</sub> concentration (mM)	pH	Time
1	Room temp (25)	7	12	30 min
2	45	7	12	30 min
3	65	7	12	30 min
4	85	7	12	30 min
5	85	1	12	30 min
6	85	2	12	30 min
7	85	3	12	30 min
8	85	4	12	30 min
9	85	5	12	30 min
10	85	6	12	30 min
11	85	7	12	30 min
12	85	8	12	30 min
13	85	9	12	30 min
14	85	10	12	30 min
15	85	20	12	30 min
16	85	10	6	30 min
17	85	10	8	30 min
18	85	10	10	30 min
19	85	10	12	30 min
20	85	10	14	30 min
21	85	10	14	10 min
22	85	10	14	30 min
23	85	10	14	60 min
24	85	10	14	2 hr
25	85	10	14	2 hr
26	85	10	14	3 hr
27	85	10	14	5 hr
28	85	10	14	24 hr
29	85	10	14	4 day

**Figure 1.** Synthesis of AgNPs at different temperatures at 7 mM AgNO<sub>3</sub>, pH = 12, and reaction time 30 min.

The lowest concentration that did not show visible growth in the wells was considered the MIC value. The reference antibiotic was itraconazole [25,26].

### 3. Results and discussions

#### 3.1. UV-vis spectroscopy

The synthesis of AgNPs was confirmed by a UV-vis spectrophotometer (300-700 nm). In the final solution, the first evidence of the formation of AgNPs ( $\text{Ag}^+ \rightarrow \text{Ag}^0$ ) in the presence of the plant extract is the alteration of color from yellow to dark brown related to surface plasmon resonance (SPR) [14]. In this study, the effects of changing the concentration of the silver nitrate solution, temperature, pH of the plant extract, and time were investigated to optimize nanoparticle synthesis. In the first stage, the effects of temperature changes (ambient temperature, 45, 65, and 85 °C) were examined during the reaction. A SPR peak centered at around 420 nm was detected for temperature changes. According to Figure 1, we can see that the highest absorption peak was with a significant difference for the temperature of 85 °C, and the lowest absorption peak was for the temperature of 45 °C, so the best and optimum temperature for the formation of AgNPs is 85 °C (Figure 1).

In the second optimization stage, the effects of the concentration of the silver nitrate solution on the increase or

decrease of the SPR peak were investigated. The synthetic reaction was carried out with different concentrations of silver nitrate (1 to 10 mM and 20 mM) (Figure 2). According to Figure 2, the best SPR peak corresponds to a concentration of 10 mM. On the other hand, with the increase in concentration, we have a shift of the SPR peaks towards a shorter wavelength (blue shift), which indicates a decrease in the size of the synthesized particles. Due to the agglomeration of nanoparticles at 20 mM of silver nitrate, the SPR peak amount has decreased compared to the concentration of 10 mM. According to the data, the optimal concentration of the silver nitrate solution for the synthesis of AgNPs is 10 mM (Figure 2).

The effects of changes in the pH of the plant extract on the SPR peak were evaluated in the next stage. The plant extract was prepared with different pH (pH: 8, 10, 12, and 14) for the synthesis steps (Figure 3). According to Figure 3, it was found that with an increase in pH from 8 to 14, we see an increase in the peak. This can be related to ionizing the phenolic functional groups in plant extract and enhancing its reduction ability [27]. No peak was observed in the synthesis at neutral pH. In addition, by changing from 12 to 14, we see a decrease in the peak shift toward shorter wavelengths (blue shift), which means that the size of the nanoparticles decreases [28]. Therefore, the best pH of the extract for the synthesis of nanoparticles by the plant is 14 (Figure 3).

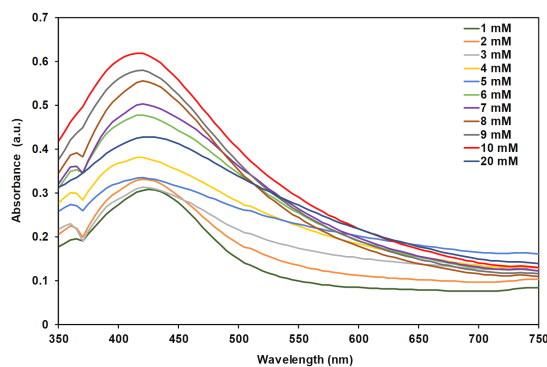


**Figure 2.** UV-vis absorption spectra of AgNPs at different concentrations of AgNO<sub>3</sub> (1-20 mM) at 85 °C, pH = 12, and reaction time 30 min.

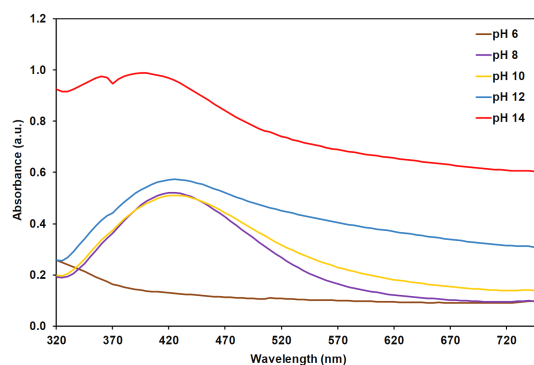


**Figure 3.** UV-vis absorption spectra of AgNPs at different pH at 85 °C, 10 mM of AgNO<sub>3</sub>, and reaction time 30 min.

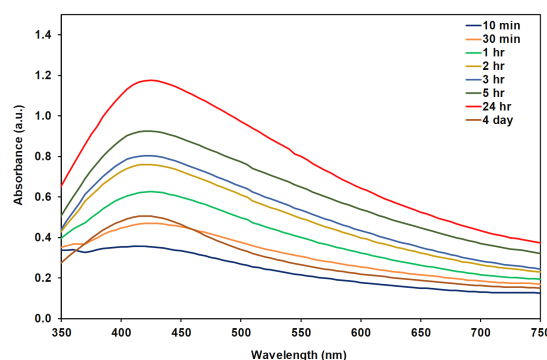


**Figure 4.** UV-vis absorption spectra of AgNPs at different reaction times at 10 mM AgNO<sub>3</sub>, pH = 14, and 85 °C.

The effects of time changes were also investigated in the last step of optimizing the synthesis of nanoparticles. It was observed that increasing the reaction time from 10 minutes to 24 hours increases the absorption peak and the average diameter of AgNPs was smaller, but the absorption peak decreases after 24 hours, indicating that the nanoparticles are larger or agglomerated (Figure 4) [15].

Studies in recent years have shown that the maximum absorption wavelength in ultraviolet (UV) is directly related to the size of the synthesized particles. Also, the shift of the absorption wavelength towards lower numbers, the blue shift, shows the reduction of the size of the nanoparticles in the optimization [13,15,29], and the attained UV spectra demonstrated that the red shift occurred by the increased size of nanoparticles [4]. Therefore, the best condition for the green synthesis of AgNP using *N. pogonosperm* was determined to be 10 mM AgNO<sub>3</sub>, pH = 14, temperature 85 °C, and reaction time 24 hours.

### 3.2. XRD, EDX, FESEM, DLS, Zeta potential, and FT-IR analysis

The XRD pattern of the prepared biosilver nanoparticles is shown in Figure 5. The XRD spectrum of the obtained AgNPs showed a very small amount of impurity because the absence of another characteristic peak indicates the absence of impurities in the obtained AgNPs [15]. 2 $\theta$  peaks at 38.22, 44.32, 64.59 and 77.5° related to the lattice planes of the face-centered cubic crystal structure of AgNPs in (111), (200), (220) and (311) (Figure 5), respectively (matched with JCPDS file no. 0783-04-04). Using the Scherer equation ( $d = 0.9 \lambda / \beta \cos \theta$ , where  $\lambda$  is the wavelength of the X-ray,  $\beta$  is the full width at half maximum (FWHM) and  $\theta$  is the diffraction angle) [30], the average size of the bio-prepared AgNPs was 31.68 nm. In parallel studies conducted in 2020 and 2022 by Shirzadi Ahodashti *et al.* and Hashemi *et al.*, the results obtained from XRD indicated that the synthesized green AgNPs have a cubic crystal structure with high purity, which is similar to the results obtained from our XRD analysis data [11,15].

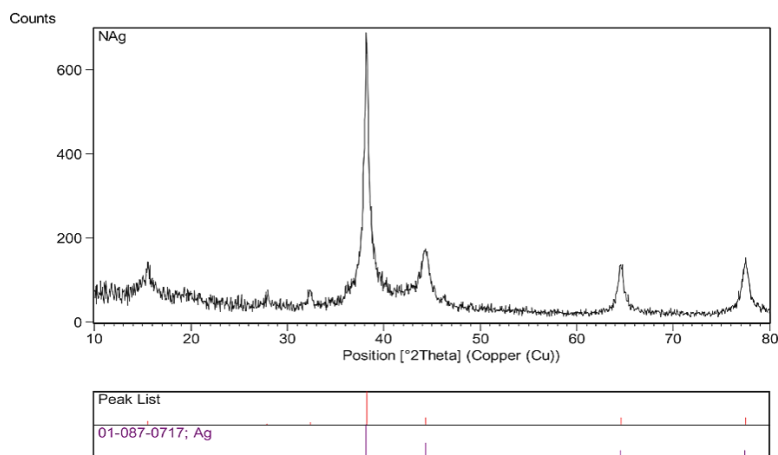


Figure 5. The XRD pattern of AgNPs synthesized by the *N. pogosperma* plant.

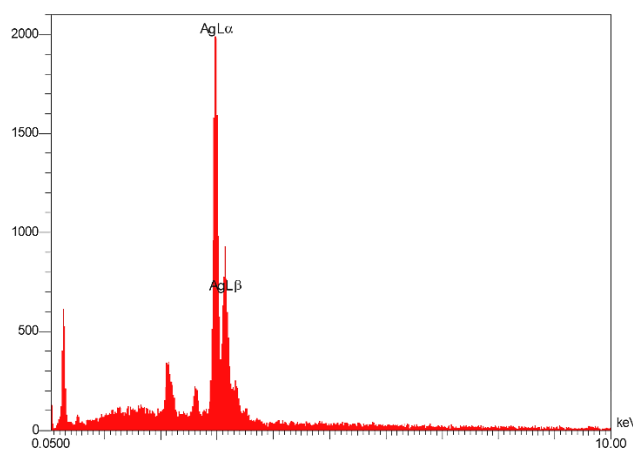


Figure 6. The EDX pattern is related to AgNPs synthesized by the *N. pogosperma* plant.

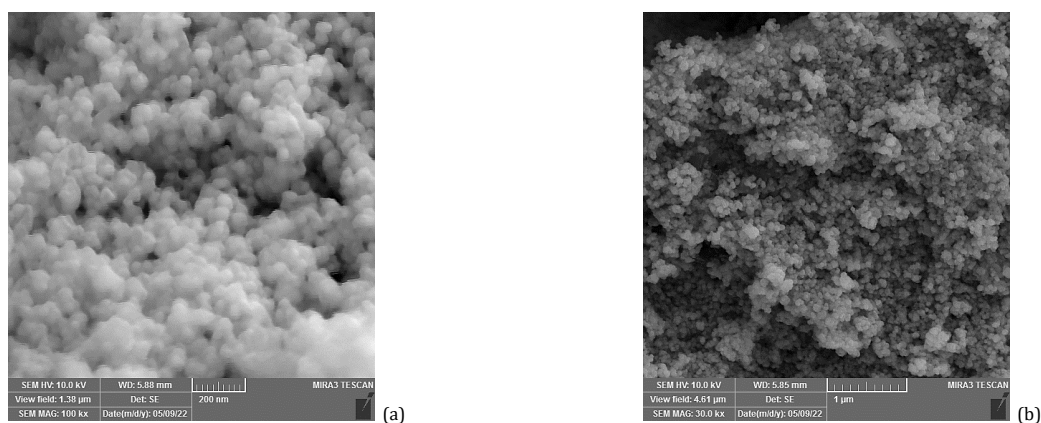


Figure 7. The FESEM micrograph of AgNPs prepared by the *N. pogosperma* plant at 200 nm (a) and 1  $\mu$ m (b).

The elemental analysis (EDX) profile of AgNPs synthesized by the plant showed strong signals from silver in the region of about 3 keV, along with weak peaks of carbon and oxygen in the region of 0.28 and 0.53 keV, as shown in Figure 6. Carbon and oxygen peaks may originate from biomolecules in the plant extract attached to the surface of AgNPs, and they play an essential role in the synthesis and stabilization of bio prepared AgNPs [31]. The EDX analysis of *S. officinale* leaf extract-mediated AgNPs showed the highest peak at 3 keV [32].

The morphology of AgNPs was analyzed by FESEM images (Figure 7). Most of the particles were spherical, and some were

oval. The biosynthesized AgNPs have shown a proper dispersion in the images. On the basis of the images, the average size of biosynthesized nanoparticles was measured  $51.21 \pm 0.02$  nm. The histogram obtained from the SEM micrograph presented the size range of the synthesized NPs, as shown in Figure 8. One of the effective factors in the size change in the NPs is related to the presence of biomolecules from the plant extract that are attached to the surface of the NPs [33]. In addition, the larger size of Ag may be due to aggregation of smaller particles [34].

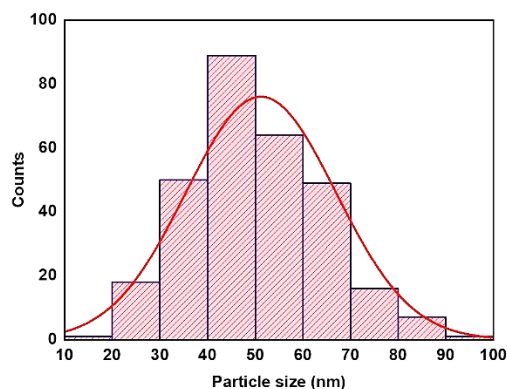


Figure 8. The Histogram of AgNPs prepared by the *N. pogonosperma* plant.

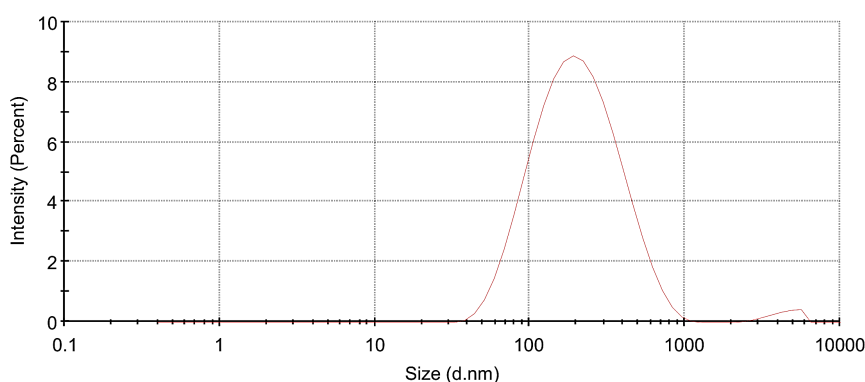


Figure 9. The DLS diagram of Ag NPs prepared by the *N. pogonosperma* plant.

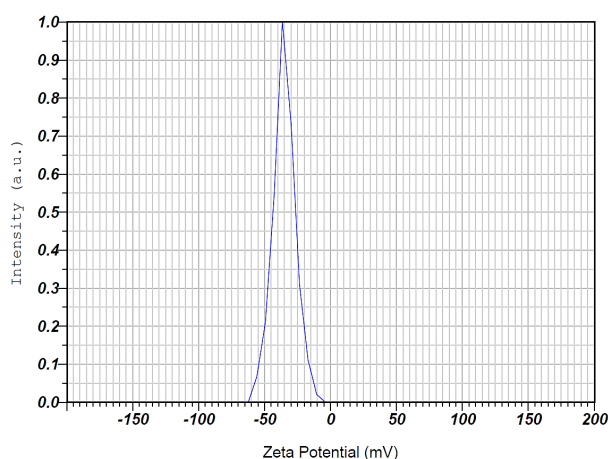


Figure 10. The zeta potential of AgNPs prepared by the *N. pogonosperma* plant.

Figure 9 presents the DLS pattern of the AgNP suspension prepared using the aqueous extract of *N. pogonosperma*. The DLS analysis showed a size of 233 nm for AgNPs, which was significantly larger than that predicted by TEM measurements. This variance might be caused by the adsorption of water on the surface of AgNPs, the aggregation of some small particles, and the adsorption of organic stabilizers from the extract; all of these might have a negative effect on the average particle size prediction using the DLS [35]. In addition, the polydispersity index (PDI) was determined to be 0.293 for the prepared AgNPs.

The zeta potential of the biosynthesized AgNPs was -35.1 mV (Figure 10), confirming the interaction of AgNPs with existing biomolecules in the extract. As a result, there are

repulsive forces between negatively charged Ag NPs, creating the moderate stability of the suspension. The zeta potential of *E. japonica* leaf extract-mediated Ag NPs was -34 mV [35].

FTIR spectroscopy (Figure 11) can help identify the potential functional groups involved in stabilizing and reducing Ag NPs produced by green synthesis. Figure 11 shows the results of an FT-IR examination of the extract and the AgNPs produced. The results showed that the FT-IR spectra of the extract and as-synthesized NPs were reasonably similar, with a few minor shifts. The AgNP spectrum indicated peaks at 3263, 2919, 2852, 1599, 1514, and 1022  $\text{cm}^{-1}$ . The peak at 3247  $\text{cm}^{-1}$  was attributed to O-H stretching vibration, and the peaks at 2919 and 2852  $\text{cm}^{-1}$  were related to C-H stretching vibrations.

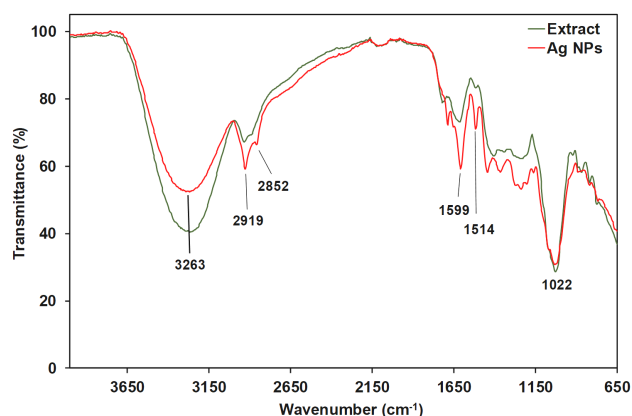
**Table 2.** MIC and MBC values for AgNPs against bacterial strains.

Bacteria	ATCC	AgNPs		Extract MIC ( $\mu\text{g/mL}$ )	Ciprofloxacin MIC ( $\mu\text{g/mL}$ )
		MIC ( $\mu\text{g/mL}$ )	MBC ( $\mu\text{g/mL}$ )		
<i>S. aureus</i>	ATCC 29213	2.34	18.75	>2500	0.21
<i>E. faecalis</i>	ATCC 29212	2.34	4.7	>2500	0.21
<i>P. aeruginosa</i>	ATCC 27853	1.17	2.34	>2500	0.3
<i>A. baumannii</i>	ATCC 19606	1.17	1.17	>2500	0.25
<i>E. coli</i>	ATCC 25922	1.17	2.34	>2500	0.1
<i>K. pneumoniae</i>	ATCC 700603	2.34	4.7	>2500	0.1
<i>P. mirabilis</i>	ATCC 25933	2.34	4.7	>2500	0.1

**Table 3.** MIC and MBC results of synthesized AgNPs against clinically resistant bacterial strains\*.

Bacteria	AgNPs		Extract MIC ( $\mu\text{g/mL}$ )	Susceptibility to antibacterial agents*											
	MIC ( $\mu\text{g/mL}$ )	MBC ( $\mu\text{g/mL}$ )		M	V	O	T	G	P	CI	CE	E	CM	AK	
<i>S. aureus</i> (VRSA)	2.34	4.7	>2500	R	R	R	S	R	R	R	R	R	R	R	R
<i>S. aureus</i> (MRSA)	4.7	4.7	>2500	R	R	R	S	R	R	R	R	R	R	R	R
<i>E. faecalis</i>	2.34	4.7	>2500	S	R	R	R	R	R	S	R	R	R	R	R
<i>P. aeruginosa</i>	2.34	9.4	>2500	R	R	R	R	R	R	R	R	R	R	R	R
<i>A. baumannii</i>	2.34	4.7	>2500	R	R	R	R	R	R	R	R	R	R	R	R
<i>E. coli</i>	4.7	4.7	>2500	R	R	R	R	R	R	R	R	R	R	R	R
<i>K. pneumoniae</i>	4.7	18.75	>2500	R	R	R	R	R	R	R	R	R	R	R	R
<i>P. mirabilis</i>	9.4	9.4	>2500	R	R	R	R	R	R	R	R	R	R	R	R

\* Bacterial strains: R, resistant; S, susceptible; M: Methicillin; V: Vancomycin; O: Oxacillin; T: Tetracycline; G: Gentamicin; P: Penicillin; CI: Ciprofloxacin; CE: Ceftazidime; E: Erythromycin; CM: Clindamycin; A: Amikacin; MRSA: Methicillin resistant *Staphylococcus aureus*; VRSA: Vancomycin resistant *Staphylococcus aureus*.

**Figure 11.** The FT-IR analysis of AgNPs synthesized by the *N. pogonosperma* plant.

These peaks are present following the levels of the polyphenolic component and other substances, such as the carbohydrates of amides. In addition, stretching vibrations of C=C and -C-O were observed at 1599 and 1022  $\text{cm}^{-1}$ . Polyphenols are considered critical phytochemicals involved in the metallic reduction. Therefore, the extracted compounds play the reducing, stabilizing, and capping roles in the biosynthesis of AgNPs. The generated AgNPs can further be functionalized, for instance, as a drug carrier, using a stabilizing coating [28,30,36].

### 3.3. Antibacterial activity evaluation

The antibacterial activity of AgNPs against selected Gram-positive and negative bacteria was investigated using the microbroth dilution method [25]. MIC and MBC ( $\mu\text{g/mL}$ ) values ( $\text{g/mL}$ ) for AgNP synthesized were measured in several ATCC strains (Table 2) and some hospital isolated strains that were resistant to some antibiotics (Table 3).

According to the determined values for the MIC and MBC values, green AgNPs exhibited a strong antibacterial effect against all bacteria. Furthermore, they showed a better inhibitory effect against *P. aeruginosa*, *A. baumannii*, and *E. coli* (MIC = 1.17  $\mu\text{g/mL}$ ), and these effects were observed in other strains of ATCC bacteria with a slightly lower effect (MIC = 2.34  $\mu\text{g/mL}$ ). The values obtained were excellent compared to the reference antibiotic. Also, the MBC results obtained from

investigating the antibacterial effects of biosynthesized AgNPs showed that the lethal effects of these nanoparticles are very significant and impressive. In general, the results of resistant bacteria isolated from hospital and biosynthesized AgNPs have shown potential effects on these resistant strains. The MIC value for AgNPs against *S. aureus* (VRSA), *P. aeruginosa*, and *A. baumannii* was 2.34  $\mu\text{g/mL}$  and also against *S. aureus* (MRSA), *E. coli*, and *K. pneumoniae*, was 4.7  $\mu\text{g/mL}$ . The silver nanoparticles exhibited a MIC of 9.4  $\mu\text{g/mL}$  on *P. mirabilis*. The antibacterial activity of plant extracts alone was also investigated on the tested bacterial strains, and plant extracts with a very high concentration (up to the concentration of 2500  $\mu\text{g/mL}$ ) had no inhibitory effect on bacteria.

There are various hypotheses for the antibacterial effects of silver nanoparticles, the most important of which is that the binding of silver ions as a result of their positive charge (time of dissolution in liquids) and their binding to the bacterial cell wall has a negative charge, and as a result, the destruction of the bacterial cell wall possibly occurs. Furthermore, in bacteria, there are sulfhydryl groups in different parts, such as enzymes, which positively charged silver ions prevent the growth of bacteria by binding to them [4,37]. In a study published in 2020, Rokonujaman Khan and colleagues evaluated the antimicrobial activity of AgNPs synthesized using the leaf extract of *Ipomoea aquatica*. The results showed that these nanoparticles have a good antimicrobial effect against *E. coli*, *Salmonella*, and *Staphylococcus sp* [38].

**Table 4.** The MIC value achieved from the biosynthesized AgNPs against several fungi isolates.

Fungi isolates tasted	AgNPs	Itraconazole	Extract
	MIC (µg/mL)	MIC (µg/mL)	MIC (µg/mL)
<i>A. fumigatus</i> (IFRC 1649)	0.585	≥16	>2500
<i>A. fumigatus</i> (IFRC 1505)	0.585	≥16	>2500
<i>T. mentagrophytes</i> (FR1 22130)	1.170	≥16	>2500
<i>T. mentagrophytes</i> (FR5 22130)	0.585	≥16	>2500
<i>F. proliferatum</i> (IFRC 1871)	0.146	≥16	>2500
<i>F. equiseti</i> (IFRC 1872)	2.340	≥16	>2500
<i>C. albicans</i> (IFRC 1873)	0.073	≥16	>2500
<i>C. albicans</i> (IFRC 1874)	0.073	≥16	>2500

In another study in 2021 on multidrug resistant bacteria, green AgNPs prepared with *Syzygium aromaticum* extract (clove) had a good inhibitory effect against *Pseudomonas aeruginosa* (D31), *Klebsiella pneumoniae* (DF30), *Klebsiella pneumoniae* (B45) and *Staphylococcus aureus* (W35) [39].

### 3.4. Antifungal activity evaluation

The antifungal activity of AgNPs was performed by the broth microdilution method [25]. The results showed that the prepared AgNPs have great inhibitory effects on fungal strains (Table 4). Meanwhile, the best inhibitory effect was observed against strains of *C. albicans* with a MIC value of 0.073 µg/mL and the lowest inhibitory effect against strain *F. equiseti* with a MIC value of 2.34 µg/mL. Furthermore, AgNPs indicated MIC values of 0.146 µg/mL for IFRC 1871, 0.585 µg/mL for IFRC 1649, FR5 22130 and IFRC 1505, and 1.17 µg/mL for FR1 22130 (Table 4).

The effectiveness of synthesized metal nanoparticles against microorganisms and multidrug resistance strongly depends on the physical and chemical properties of the synthesized nanoparticles, such as size, shape, surface charge, and size distribution [40,41]. In general, the results showed that the synthesized NPs had extremely significant effects on all fungal strains compared to itraconazole (positive control). Similarly, to the antibacterial mechanism of AgNP, some of the antifungal mechanisms of these NPs include adhesion to the fungal membrane, affecting the levels of ergosterol and fatty acids, reducing membrane fluidity, DNA damage, and ROS production (reactive oxygen species) [42]. In 2020, AgNPs synthesized using *Melia azedarach* leaf extract showed good effects against *Verticillium dahlia*, *Colletotrichum coccodes*, *Monilinia sp*, and *Pyricularia sp* under both *in vitro* and *in vivo* conditions [43]. Alsayed E. Mekky and colleagues in 2021, AgNPs prepared from *Spinacia oleracea* leaves showed a good inhibitory effect on fungal strains *Aspergillus niger*, *Talaromyces marneffie*, *Candida glabrata* and *Candida parapsilosis*, and the measured MIC for all species was 8 µg/mL [44]. In an article published in 2020, photosynthesized SNPs from *Ferulago macrocarpa* flower extract also exhibited significant antifungal activity against *Candida albicans* with a minimum fungicidal concentration (MFC) value of 500 µg/mL [45].

## 4. Conclusions

With the increasing population and the development of multiple drug resistance in various pathogens and microorganisms, we need a way to overcome this issue. Green nanoparticle synthesis using plants is the best, most environmentally friendly, safe, and affordable method. The optimal conditions for the synthesis of AgNPs were determined to be 10 mM AgNO<sub>3</sub>, pH = 14, temperature 85 °C, and reaction time 24 hours. AgNPs were synthesized using *N. pogonosperma*, and characterized by instrumental analysis techniques, including X-ray diffraction (XRD), EDX, FESEM, FT-IT, DLS, Zeta potential, and UV-Vis. The nanoparticles were spherical, with an average particle size of 51.21±0.02. Additionally, Ag NPs had a potential antibacterial effect against strains of *P. aeruginosa*, *A.*

*baumannii*, and *E. coli* (MIC = 1.17 µg/mL). The biosynthesized AgNPs in this study indicated amazing antifungal effects against various resistant strains, especially strains of *C. albicans* (0.073 µg/mL), which is significant compared to Itraconazole (MIC ≥16 µg/mL) as a positive control.

## Acknowledgements

This study was carried out with the financial support of the Research Council of the Mazandaran University of Medical Sciences. (IR.MAZUMS.REC.1400.11446).

## Disclosure statement


Conflict of interest: The authors declare that they have no conflict of interest. Ethical approval: All ethical guidelines have been adhered to. Sample availability: Samples of the compounds are available from the author.

## CRedit authorship contribution statement

Conceptualization: Amin Barani, Seyedeh Roya Alizadeh, Mohammad Ali Ebrahimzadeh; Methodology: Amin Barani, Mohammad Ali Ebrahimzadeh, Hamid Reza Goli, Amir Hossein Habibian; Formal analysis: Amin Barani, Seyedeh Roya Alizadeh; Investigation: Amin Barani, Mohammad Ali Ebrahimzadeh, Amir Hossein Habibian; Resources: Seyedeh Roya Alizadeh; Funding: Seyedeh Roya Alizadeh; Supervision: Seyedeh Roya Alizadeh; Writing - Original Draft: Amin Barani, Mohammad Ali Ebrahimzadeh, Hamid Reza Goli, Seyedeh Roya Alizadeh; Review and Editing: Seyedeh Roya Alizadeh.


## ORCID and Email

Mohammad Ali Ebrahimzadeh

 [zadeh20@gmail.com](mailto:zadeh20@gmail.com)


 <https://orcid.org/0000-0002-8769-9912>


Amin Barani

 [justallah2021@gmail.com](mailto:justallah2021@gmail.com)

 <https://orcid.org/0000-0002-5299-6044>

Amir Hossein Habibian

 [iamirhossein97@gmail.com](mailto:iamirhossein97@gmail.com)

 <https://orcid.org/0000-0003-1633-5174>

Hamid Reza Goli

 [goli59@gmail.com](mailto:goli59@gmail.com)

 <https://orcid.org/0000-0002-2932-1911>

Seyedeh Roya Alizadeh

 [r.alizadeh.2019@gmail.com](mailto:r.alizadeh.2019@gmail.com)

 [ro.alizadeh@mazums.ac.ir](mailto:ro.alizadeh@mazums.ac.ir)

 <https://orcid.org/0000-0001-7435-4635>

## References

- [1]. Sbaraglini, M. L.; Talevi, A. Hybrid compounds as anti-infective agents. *Curr. Top. Med. Chem.* **2017**, *17*, 1080-1095.
- [2]. Mba, I. E.; Nweze, E. I. Nanoparticles as therapeutic options for treating multidrug-resistant bacteria: research progress, challenges, and prospects. *World J. Microbiol. Biotechnol.* **2021**, *37*, 108.
- [3]. Borgio, J. F.; Rasdan, A. S.; Sonbol, B.; Alhamid, G.; Almandil, N. B.; AbdulAzeez, S. Emerging status of multidrug-resistant bacteria and fungi in the Arabian Peninsula. *Biology (Basel)* **2021**, *10*, 1144.
- [4]. Ebrahimzadeh, M. A.; Hashemi, Z.; Mohammadyan, M.; Fakhar, M.; Mortazavi-Derazkola, S. In vitro cytotoxicity against human cancer cell lines (MCF-7 and AGS), antileishmanial and antibacterial activities of



- green synthesized silver nanoparticles using *Scrophularia striata* extract. *Surf. Interfaces* **2021**, *23*, 100963.
- [5]. Choi, J. S.; Jung, H. C.; Baek, Y. J.; Kim, B. Y.; Lee, M. W.; Kim, H. D.; Kim, S. W. Antibacterial activity of green-synthesized silver nanoparticles using *Areca catechu* extract against antibiotic-resistant bacteria. *Nanomaterials (Basel)* **2021**, *11*, 205.
- [6]. Wertheimer, A. The urgent need for new antibiotics. *J. Pharm. Health Serv. Res.* **2022**, *13*, 167–167.
- [7]. Vivas, R.; Barbosa, A. A. T.; Dolabela, S. S.; Jain, S. Multidrug-resistant bacteria and alternative methods to control them: An overview. *Microb. Drug Resist.* **2019**, *25*, 890–908.
- [8]. Lei, Z.; Karim, A. The challenges and applications of nanotechnology against bacterial resistance. *J. Vet. Pharmacol. Ther.* **2021**, *44*, 281–297.
- [9]. Hashemi, Z.; Shirzadi-Ahodashi, M.; Ebrahimzadeh, M. A. Antileishmanial and antibacterial activities of biologically synthesized silver nanoparticles using *Alcea rosea* extract (AR-AgNPs). *J. Water Environ. Nanotechnol.* **2021**, *6*, 265–276.
- [10]. Ebrahimzadeh, M. A.; Naghizadeh, A.; Amiri, O.; Shirzadi-Ahodashi, M.; Mortazavi-Derazkola, S. Green and facile synthesis of Ag nanoparticles using *Crataegus pentagyna* fruit extract (CP-AgNPs) for organic pollution dyes degradation and antibacterial application. *Bioorg. Chem.* **2020**, *94*, 103425.
- [11]. Hashemi, Z.; Shirzadi-Ahodashi, M.; Mortazavi-Derazkola, S.; Ebrahimzadeh, M. A. Sustainable biosynthesis of metallic silver nanoparticles using barberry phenolic extract: Optimization and evaluation of photocatalytic, in vitro cytotoxicity, and antibacterial activities against multidrug-resistant bacteria. *Inorg. Chem. Commun.* **2022**, *139*, 109320.
- [12]. Hashemi, Z.; Mortazavi-Derazkola, S.; Biparva, P.; Goli, H. R.; Sadeghian, F.; Kardan, M.; Rafiei, A.; Ebrahimzadeh, M. A. Green synthesized silver nanoparticles using *Feijoa sellowiana* leaf extract, evaluation of their antibacterial, anticancer and antioxidant activities. *Iran. J. Pharm. Res.* **2020**, *19*, 306–320.
- [13]. Shirzadi-Ahodashi, M.; Mizwari, Z. M.; Hashemi, Z.; Rajabalipour, S.; Ghoreishi, S. M.; Mortazavi-Derazkola, S.; Ebrahimzadeh, M. A. Discovery of high antibacterial and catalytic activities of biosynthesized silver nanoparticles using *C. fruticosus* (CF-AgNPs) against multi-drug resistant clinical strains and hazardous pollutants. *Environ. Technol. Innov.* **2021**, *23*, 101607.
- [14]. Hashemi, Z.; Ebrahimzadeh, M. A.; Biparva, P.; Mortazavi-Derazkola, S.; Goli, H. R.; Sadeghian, F.; Kardan, M.; Rafiei, A. Biogenic silver and zero-valent iron nanoparticles by *Feijoa*: Biosynthesis, characterization, cytotoxic, antibacterial and antioxidant activities. *Anticancer Agents Med. Chem.* **2020**, *20*, 1673–1687.
- [15]. Shirzadi-Ahodashi, M.; Mortazavi-Derazkola, S.; Ebrahimzadeh, M. A. Biosynthesis of noble metal nanoparticles using *crataegus monogyna* leaf extract (CML@X-NPs, X= Ag, Au): Antibacterial and cytotoxic activities against breast and gastric cancer cell lines. *Surf. Interfaces* **2020**, *21*, 100697.
- [16]. Alizadeh, S. R.; Ebrahimzadeh, M. A. Characterization and anticancer activities of green synthesized CuO nanoparticles, A review. *Anticancer Agents Med. Chem.* **2021**, *21*, 1529–1543.
- [17]. Ouerghi, O.; Geesi, M. H.; Riadi, Y.; Ibnouf, E. O. Limon-citrus extract as a capping/reducing agent for the synthesis of titanium dioxide nanoparticles: characterization and antibacterial activity. *Green Chem. Lett. Rev.* **2022**, *15*, 483–490.
- [18]. Silva, A. A.; Sousa, A. M. F.; Furtado, C. R. G.; Carvalho, N. M. F. Green magnesium oxide prepared by plant extracts: synthesis, properties and applications. *Materials Today Sustainability* **2022**, *20*, 100203.
- [19]. Eltaweil, A. S.; Fawzy, M.; Hosny, M.; Abd El-Monaem, E. M.; Tamer, T. M.; Omer, A. M. Green synthesis of platinum nanoparticles using *Atriplex halimus* leaves for potential antimicrobial, antioxidant, and catalytic applications. *Arab. J. Chem.* **2022**, *15*, 103517.
- [20]. Sargazi, A.; Barani, A.; Heidari Majd, M. Synthesis and apoptotic efficacy of biosynthesized silver nanoparticles using acacia luciana flower extract in MCF-7 breast cancer cells: Activation of Bak1 and bclx for cancer therapy. *Bionanoscience* **2020**, *10*, 683–689.
- [21]. Ali, T.; Javan, M.; Sonboli, A.; Semnianian, S. Evaluation of the antinociceptive and anti-inflammatory effects of essential oil of *Nepeta pogonosperma* Jamzad et Assadi in rats. *Daru* **2012**, *20*, 48.
- [22]. Jamzad, Z.; Grayer, R. J.; Kite, G. C.; Simmonds, M. S. J.; Ingrouille, M.; Jalili, A. Leaf surface flavonoids in Iranian species of *Nepeta* (Lamiaceae) and some related genera. *Biochem. Syst. Ecol.* **2003**, *31*, 587–600.
- [23]. Takeda, Y.; Matsumoto, T.; Oiso, Y.; Honda, G.; Tabata, M.; Fujita, T.; Otsuka, H.; Sezik, E.; Yesilada, E. Nepetacilioside, a New Iridoid Glucoside from *Nepeta cilicia*. *J. Nat. Prod.* **1996**, *59*, 518–519.
- [24]. Fraga, B. M.; Hernández, M. G.; Mestres, T.; Arteaga, J. Abietane diterpenes from *Nepeta teydea*. *Phytochemistry* **1998**, *47*, 251–254.
- [25]. Alizadeh, S. R.; Seyedabadi, M.; Montazeri, M.; Khan, B. A.; Ebrahimzadeh, M. A. Allium paradoxum extract mediated green synthesis of SeNPs: Assessment of their anticancer, antioxidant, iron chelating activities, and antimicrobial activities against fungi, ATCC bacterial strains, Leishmania parasite, and catalytic reduction of methylene blue. *Mater. Chem. Phys.* **2023**, *296*, 127240.
- [26]. Shirzadi-Ahodashi, M.; Mizwari, Z. M.; Jafarkhani, B.; Mohamadzadeh, S.; Abbastabar, M.; Motafeghi, F.; Sadeghi Lalerdi, F.; Ali Ebrahimzadeh, M.; Mortazavi-Derazkola, S. Biogenic synthesis of spherical-shaped noble metal nanoparticles using *Vicia faba* extract (X@VF, X = Au, Ag) for photocatalytic degradation of organic hazardous dye and their in vitro antifungal, antibacterial and anticancer activities. *Inorg. Chem. Commun.* **2022**, *146*, 110042.
- [27]. Shafey, A. M. E. Green synthesis of metal and metal oxide nanoparticles from plant leaf extracts and their applications: A review. *Green Process. Synth.* **2020**, *9*, 304–339.
- [28]. Shirzadi-Ahodashi, M.; Hashemi, Z.; Mortazavi, Y.; Khormali, K.; Mortazavi-Derazkola, S.; Ebrahimzadeh, M. A. Discovery of high antibacterial and catalytic activities against multi-drug resistant clinical bacteria and hazardous pollutants by biosynthesis of silver nanoparticles using *Stachys inflata* extract (AgNPs@SI). *Colloids Surf. A Physicochem. Eng. Asp.* **2021**, *617*, 126383.
- [29]. Nikaeen, G.; Yousefinejad, S.; Rahmdel, S.; Samari, F.; Mahdavinia, S. Central composite design for optimizing the biosynthesis of silver nanoparticles using *Plantago major* extract and investigating antibacterial, antifungal and antioxidant activity. *Sci. Rep.* **2020**, *10*, 9642.
- [30]. Pirtarighat, S.; Ghannadnia, M.; Baghshahi, S. Green synthesis of silver nanoparticles using the plant extract of *Salvia spinosa* grown in vitro and their antibacterial activity assessment. *J. Nanostructure Chem.* **2019**, *9*, 1–9.
- [31]. Hashemi, Z.; Mizwari, Z. M.; Mohammadi-Aghdam, S.; Mortazavi-Derazkola, S.; Ali Ebrahimzadeh, M. Sustainable green synthesis of silver nanoparticles using *Sambucus ebulus* phenolic extract (AgNPs@SEE): Optimization and assessment of photocatalytic degradation of methyl orange and their in vitro antibacterial and anticancer activity. *Arab. J. Chem.* **2022**, *15*, 103525.
- [32]. Singh, H.; Du, J.; Singh, P.; Yi, T. H. Role of green silver nanoparticles synthesized from *Symphytum officinale* leaf extract in protection against UVB-induced photoaging. *J. Nanostructure Chem.* **2018**, *8*, 359–368.
- [33]. Gomathi, A. C.; Xavier Rajarathinam, S. R.; Mohammed Sadiq, A.; Rajeshkumar, S. Anticancer activity of silver nanoparticles synthesized using aqueous fruit shell extract of *Tamarindus indica* on MCF-7 human breast cancer cell line. *J. Drug Deliv. Sci. Technol.* **2020**, *55*, 101376.
- [34]. Sadeghi, B.; Gholamhoseinpoor, F. A study on the stability and green synthesis of silver nanoparticles using *Ziziphora tenuior* (Zt) extract at room temperature. *Spectrochim. Acta A Mol. Biomol. Spectrosc.* **2015**, *134*, 310–315.
- [35]. Rao, B.; Tang, R.-C. Green synthesis of silver nanoparticles with antibacterial activities using aqueous *Eriobotrya japonica* leaf extract. *Adv. Nat. Sci. Nanosci. Nanotechnol.* **2017**, *8*, 015014.
- [36]. Salayová, A.; Bedlovičová, Z.; Daneu, N.; Baláž, M.; Lukáčová Bujňáková, Z.; Balážová, L.; Tkáčiková, L. Green synthesis of silver nanoparticles with antibacterial activity using various medicinal plant extracts: Morphology and antibacterial efficacy. *Nanomaterials (Basel)* **2021**, *11* (4), 1005.
- [37]. Shaaban, M. T.; Ghaly, M. F.; Fahmi, S. M. Antibacterial activities of hexadecanoic acid methyl ester and green-synthesized silver nanoparticles against multidrug-resistant bacteria. *J. Basic Microbiol.* **2021**, *61*, 557–568.
- [38]. Khan, M. R.; Hoque, S. M.; Hossain, K. F. B.; Siddique, M. A. B.; Uddin, M. K.; Rahman, M. M. Green synthesis of silver nanoparticles using *Ipomoea aquatica* leaf extract and its cytotoxicity and antibacterial activity assay. *Green Chem. Lett. Rev.* **2020**, *13*, 303–315.
- [39]. Ajitha, B.; Reddy, Y. A. K.; Lee, Y.; Kim, M. J.; Ahn, C. W. Biomimetic synthesis of silver nanoparticles using *Syzygium aromaticum* (clove) extract: Catalytic and antimicrobial effects: Synthesis of Silver Nanoparticles: Catalytic and Antimicrobial Effects. *Appl. Organomet. Chem.* **2019**, *33*, e4867.
- [40]. Das, B.; Dash, S. K.; Mandal, D.; Ghosh, T.; Chattopadhyay, S.; Tripathy, S.; Das, S.; Dey, S. K.; Das, D.; Roy, S. Green synthesized silver nanoparticles destroy multidrug resistant bacteria via reactive oxygen species mediated membrane damage. *Arab. J. Chem.* **2017**, *10*, 862–876.
- [41]. Lakkim, V.; Reddy, M. C.; Pallavali, R. R.; Reddy, K. R.; Reddy, C. V.; Inamuddin; Bilgrami, A. L.; Lomada, D. Green synthesis of silver nanoparticles and evaluation of their antibacterial activity against multidrug-resistant bacteria and wound healing efficacy using a Murine model. *Antibiotics (Basel)* **2020**, *9*, 902.
- [42]. Mare, A. D.; Ciurea, C. N.; Man, A.; Mareş, M.; Toma, F.; Berta, L.; Tanase, C. In vitro antifungal activity of silver nanoparticles biosynthesized with beech bark extract. *Plants* **2021**, *10*, 2153.
- [43]. Jebri, S.; Khanfir Ben Jenana, R.; Dridi, C. Green synthesis of silver nanoparticles using *Melia azedarach* leaf extract and their antifungal activities: In vitro and in vivo. *Mater. Chem. Phys.* **2020**, *248*, 122898.

- [44]. Mekky, A.; Farrag, A.; Sofy, A.; Hamed, A. Antibacterial and Antifungal Activity of Green-synthesized Silver Nanoparticles Using Spinacia oleracea leaves Extract. *Egypt. J. Chem.* **2021**, 64 (10), 5781–5792.
- [45]. Azarbani, F.; Shiravand, S. Green synthesis of silver nanoparticles by *Ferulago macrocarpa* flowers extract and their antibacterial, antifungal and toxic effects. *Green Chem. Lett. Rev.* **2020**, 13, 41–49.



Copyright © 2023 by Authors. This work is published and licensed by Atlanta Publishing House LLC, Atlanta, GA, USA. The full terms of this license are available at <http://www.eurjchem.com/index.php/eurjchem/pages/view/terms> and incorporate the Creative Commons Attribution-Non Commercial (CC BY NC) (International, v4.0) License (<http://creativecommons.org/licenses/by-nc/4.0>). By accessing the work, you hereby accept the Terms. This is an open access article distributed under the terms and conditions of the CC BY NC License, which permits unrestricted non-commercial use, distribution, and reproduction in any medium, provided the original work is properly cited without any further permission from Atlanta Publishing House LLC (European Journal of Chemistry). No use, distribution, or reproduction is permitted which does not comply with these terms. Permissions for commercial use of this work beyond the scope of the License (<http://www.eurjchem.com/index.php/eurjchem/pages/view/terms>) are administered by Atlanta Publishing House LLC (European Journal of Chemistry).